Turkish Journal of Electrical Engineering & Computer Sciences

http://journals.tubitak.gov.tr/elektrik/

Research Article

Turk J Elec Eng & Comp Sci
(2017) 25: 2749 – 2760

doi:10.3906/elk-1606-191

Robust seed detection for coronary arteries segmentation using thresholded Frangi response

Sammer ZAI[1], Muhammad Ahsan ANSARI[1], Soon-Young SONG[2], Young Shik MOON[1,*]
[1]Department of Computer Science Engineering, Hanyang University, Ansan, South Korea
[2]Department of Radiology, College of Medicine, Hanyang University, Seoul, South Korea

Received: 13.06.2016 • **Accepted/Published Online:** 20.10.2016 • **Final Version:** 30.07.2017

Abstract: Automatic detection of initial seed points has become an essential step towards delineating coronary arteries in coronary computed tomography angiography (CCTA) images due to image inhomogeneity and other factors. Most coronary segmentation algorithms require user interaction for seed point selection, which may lead to erroneous segmentation. In this study, we present an improved technique of seed detection for coronary segmentation using a thresholded Frangi response. Before computing region of interest (ROI), the proposed method first computes the Frangi response of the complete CCTA volume, followed by thresholding with respect to quantile and median values, and then the ROI selection procedure is applied. Further, this procedure is joined with a feature that is built according to the resemblance among consecutive orthogonal cross-sections. The proposed method was evaluated on nine clinical datasets, and the proposed framework automatically detected coronary seeds accurately and can be used for an accurate delineation of coronary arteries. The obtained results were compared qualitatively and quantitatively by a radiologist, and the proposed method outperformed the previous method with an improvement of 45.9%.

Key words: Coronary artery disease, coronary computed tomography angiography, region of interest

1. Introduction

Coronary artery disease (CAD) is one of the major causes of death worldwide in the last decade [1]. Coronary computed tomography angiography (CCTA) is one of the most popular imaging tools used for cardiovascular disease diagnosis, as it provides detailed information, including the existence of stenosis and occlusions. Compared to two-dimensional (2D) angiography, three-dimensional (3D) CCTA delivers higher accuracy in diagnoses. Despite extensive studies, the segmentation of coronary arteries from CCTA still remains a challenging task due to the presence of diverse anatomical structures surrounding the heart in cardiac CCTA data. However, most of the studies presented in the literature require one or multiple seed points for segmenting the coronary arteries. These starting seed points are provided with the help of user interaction in most cases. Manual selection of seed points by distinct users may lead to erroneous segmentation because the accuracy of the segmented coronary arteries heavily depends on the selection of starting points. This study provides a robust mechanism for the accurate detection of coronary seeds points that can be used for efficiently segmenting the coronary arteries. The presented method provides a mechanism for making the seed detection procedure automatic, which may enhance segmentation accuracy without user involvement. An accurate yet fast segmentation method is required because of the huge amount of image data and the complex structures of coronary arteries.

*Correspondence: ysmoon@hanyang.ac.kr

2. Literature review

Various methods have been presented in the literature for isolating the coronary arteries from CCTA data. However, one or several initial seed point(s) are needed by most of the methods [2–4] for the delineation of coronary arteries. In most cases, the provision of these starting seed points is accomplished with the help of user involvement, which may result in inaccurate segmentation.

To achieve an accurate segmented coronary tree based on initial seed point(s), several approaches have been proposed in the literature. Lankton et al. [4] presented an arterial tree segmentation technique based on universal modeling energy (Chan–Vese energy) as the driving force of evolving contour in region-based segmentation. Segmentation started with a single point initialized by the user. Kitslaar et al. [5] first detected the complete heart section and aorta, followed by a region-growing method that started in the aorta and halted over the points where candidate components of the coronary tree were found. The authors in [6] presented a generic approach for automatically detecting tubular objects along with the extraction of their centerlines, which were grouped together into tree structures. In [7], Kitamura et al. presented a technique based on learning a classifier of a 3D tube-shaped component with a dimension-lessening method by analyzing the Hessian matrix. Potential coronary seeds were computed by authors in [8] by approximating the heart's position, and then the coronary vessel tree was extracted by fitting the cylindrical sampling patterns. All of the above methods do not take into consideration the shape information of the coronary arteries as prior knowledge in their approaches. However, in [9], the authors utilized the benefits of shape statistics of major coronary arteries, and on the basis of this prior information they proposed an algorithm for detecting coronary seeds automatically, but the algorithm uses the Sobel operator to detect edges of the candidate ROIs, which affects the accuracy of edge detection because smoothing decreases the magnitude of edge. Since medical images are usually blurred in nature, the Sobel operator may not produce very accurate results.

To overcome this issue, the authors in [9] used morphological operations. These operations, unfortunately, remove some significant parts of coronary arteries that are very small or located at the boundary of heart region. Moreover, in [9], a Hessian-based vesselness response was taken after ROI selection to speed up the process. However, the selection of a single slice does not guarantee the presence of all parts of major coronary arteries. In that case, the authors in [9] proposed using multiple slices for detecting seeds, but computing Hessian-based vesselness for ROIs of different slices will increase processing time. Therefore, this paper proposes a framework that is efficient in terms of processing time and robust in terms of accuracy. The proposed method is different from the previous method in that it not only computes the Hessian-based vesselness prior to ROI selection procedure, but also it thresholds the Hessian-based vesselness response with respect to the quantile and median of 26 neighbors. Moreover, the proposed method does not require morphological operations, which are not more than simple cosmetics.

The paper is organized in the following order: background methods are discussed in Section 3. Section 4 describes the proposed method with example figures. Experimental results are explained in Section 5 and the performance of the proposed framework is discussed in Section 6. Lastly, Section 7 concludes this research.

3. Background methods

3.1. Hessian-based multiscale vessel enhancement

For an effective vessel enhancement, the vesselness measure proposed by Frangi et al. [10] was used to differentiate vessel-like structures from other structures. The method is based on examination of a Hessian matrix and corresponding eigenvalues for the extraction of tubular objects. After eigenvalue decomposition of

the Hessian matrix, the eigenvalues λ_1, λ_2, and λ_3 are sorted as $|\lambda_1| < |\lambda_2| < |\lambda_3|$ where $|\lambda_1| \approx 0, |\lambda_1| \ll |\lambda_2|$ and $|\lambda_2| \approx |\lambda_3|$ are the conditions for an ideal tubular structure in a 3D image. On the basis of this analysis, Frangi's vesselness measure distinguishes tube-like objects from blob-like or plate-like structures and the background. The vesselness function is defined using Eq. (1):

$$f(\sigma) = \left\{ \begin{array}{ll} 0, & if \lambda_2 > 0 | \lambda_3 > 0 \\ \left(1 - e^{-\frac{R_A^2}{2\alpha}}\right) e^{-\frac{R_B^2}{2\beta}} \left(1 - e^{-\frac{R_S^2}{2\gamma}}\right), & otherwise \end{array} \right\}, \tag{1}$$

where σ defines the scale at which vesselness is measured. The parameters α, β, and γ control the sensitivity of R_A, R_B, and R_S, respectively.

$R_A = |\lambda_2|/|\lambda_3|$, $R_B = |\lambda_1| \Big/ \sqrt{|\lambda_2 \lambda_3|}$, and $R_S = \sqrt{\sum_j \lambda_j^2}$

The term R_A describes whether the local structure is more plate-like or tube-like, the term R_B accounts for blob-like structures, and the term R_S deals with the difference between the vessel and nonvessel components. The maximum response across various scales is selected as the optimal solution using Eq. (2):

$$f(\sigma) = \max_{\sigma_{\min} \leq \sigma \leq \sigma_{\max}} f(\sigma), \tag{2}$$

where $\sigma_{\min}$ and $\sigma_{\max}$ define the minimum and maximum scales, respectively.

In CCTA images, various objects show the same intensity range as coronaries, which will easily lead to leakages when the segmentation is started with an initial surface near these objects. However, a Hessian-based multiscale vessel enhancement filter can be useful for removing these unwanted objects, since they usually exhibit blob-like structures and also have quite different features than wanted objects or the tube-like structures that are coronary arteries, but due to the same CT values in nearby objects, this method produces strong step-edge responses, which may lead to false extractions.

3.2. Seed detection

Most vessel segmentation requires seed point(s) for their further propagation. The accuracy of the segmentation method depends upon the selection of seed points. As discussed in Section 1, manual definition of seed points may lead to inaccurate segmentation. Therefore, an automatic method for seed selection is desired. One such work has been presented in [9], in which they have proposed using a local geometric feature in combination with a Hessian-based filter to detect vessel regions. In their work, first, an axial slice should be selected that contains the components of all major coronary arteries. According to them, such a slice is found nearly in the middle of the scan range, and the index P of such a selected slice is calculated using Eq. (3).

$$P = c_r \times N \tag{3}$$

Here N corresponds to the total number of slices in a given CTA volume and c_r is a constant. To reduce the dataset more, only the heart region is selected using a heart region detection technique [11], because, according to anatomical information, coronary arteries commonly exist within the heart zone. Then the ROI selection procedure is applied and the local geometric feature is computed as described in [9]. The final vesselness, based on local geometric feature and a Hessian-based filter, is computed using Eq. (4), where T_F is the threshold for Hessian-based vesselness $\mathrm{F}(x)$ and T_{GF} is the threshold for the local geometric feature $\mathrm{GF}(x)$.

$$\text{vesselness}(x) = \left\{ \begin{array}{ll} 1, & if \ F(x) \geq T_F \text{ and } GF(x) \geq T_{GF} \\ 0, & otherwise \end{array} \right\}, \tag{4}$$

where the local geometric feature GF(x) is computed using Eq. (5).

$$GF(x) = \prod_{j=1}^{10} \frac{k}{B_{\max}[j] - B_{\min}[j] + 1}, \tag{5}$$

According to Eq. (5), the local geometric feature is computed by selecting three orthogonal cross-sections in the direction of the vessel and three UV planes are acquired as the transverse cross-sections of the cylinder along the vessel direction. On each of the three selected UV planes with indices [–1, 0, 1], rays are projected along 16 evenly sampled directions from the respective center point of each plane. By using a radial gradient, the border point is detected along each ray. The rays are sorted for each of the three center points with respect to their lengths, and then the three longest and three shortest rays are discarded. The minimum and maximum values $B_{\min}[j]$ and $B_{\max}[j]$ for each ray index among the three ray lengths d[–1,0,1][j] are computed. The term k represents some constant.

The method of seed detection provides a good mechanism for detecting coronary seed points. However, this method requires the selection of an axial slice showing all three major coronary arteries using Eq. (3), which is not always guaranteed to contain all major coronaries. Moreover, the use of the Sobel operator on the obtained heart region may produce broken edges for the selected regions. Additionally, this method assumes that the vessel is cylindrical and may fail at vessel bifurcation because, generally, the vessel cross-section at the bifurcation region is not circular.

3.3. Proposed method

The proposed method is an improvement of the work described in [9]. The authors in [9] began by first finding the ROI using shape analysis. The first step in shape analysis is edge detection, for which they used the Sobel operator. The Sobel operator usually generates better results, as it is less sensitive to noise because of the smoothing operator it uses. However, this smoothing operation affects the accuracy of edge detection, as it decreases the magnitude of edge. Consequently, it leads to the problem of missing true edges. Consider an image, as shown in Figure 1a, to which region detection technique was applied for the resultant image in Figure 1b. The magnified view of the area enclosed by the yellow box in Figure 1b is shown in Figure 1c. It can be seen very clearly that the coronary artery component shown in Figure 1c looks sharp but is slightly blurred, causing Sobel edge detector failures in producing good edges, as shown in Figure 1d. Similarly, the magnified view of the region enclosed by the green box is shown in Figure 1e, and its respective image containing edges detected by the Sobel operator is shown in Figure 1f. Since the image components in Figure 1e are blurred, the edges detected by the Sobel operator are not accurate, causing Sobel edge detector failures in producing correct edges, as shown in Figure 1f.

To overcome the problems shown in Figure 1, the authors in [9] suggest using morphological operations such as dilation and opening, which are image-specific operations. Moreover, the usage of these operations may remove significant seeds of coronary arteries that are very small or that are located at the boundary of the heart region. Another limitation of the approach proposed in [9] is that the selection of only one slice is not always guaranteed to be sufficient for the selection of seeds of all major coronary arteries.

In order to avoid the limitations discussed above, we propose some improvements to the existing algorithm. The block diagrams for the original idea and the proposed idea are shown in Figures 2a and 2b, respectively. In our approach, we compute the Hessian-based vesselness of the entire volume before the ROI selection process

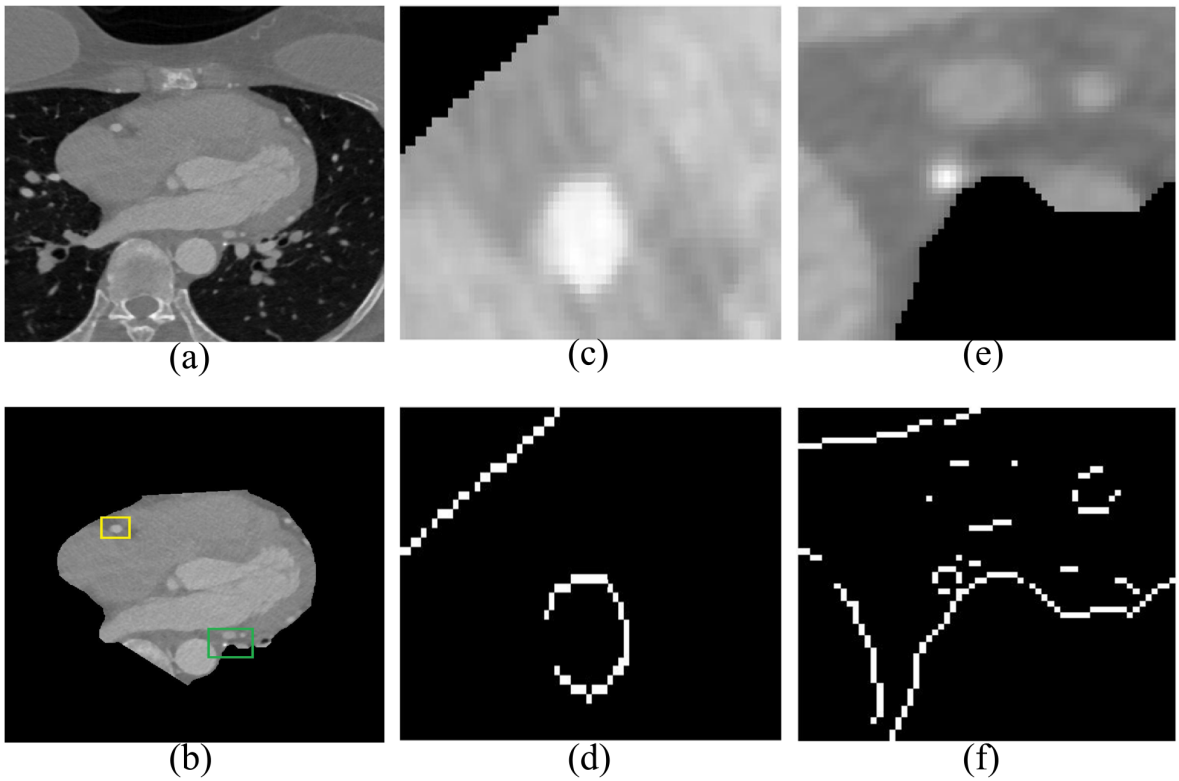

Figure 1. The response of the Sobel edge detector. (a) Original slice from CCTA. (b) Heart region using region detection technique [11]. (c) Close view of the portion marked by a yellow box in (b). (d) Sobel edge detection applied to (c). (e) Close view of the portion marked by the green box in (b). (f) Sobel edge detection applied to (e).

for accurate seed detection. The computation of Hessian-based vesselness before ROI selection will require less time, especially in the case of multiple slices to be used for seed detection.

Furthermore, we created a restricted domain that only includes voxels representing the heart and ignores all other voxels representing air. This domain is created by excluding any point that falls below a threshold of –600 Hounsfield units [4].

As reported in [12], Hessian-based vesselness usually cannot detect vessel features accurately for boundary pixels, and the vessel components at the boundary of vessels may become a bit narrower in comparison with the original one. An example CCTA image portion of such a case is shown in Figure 3a, whose Sobel edge detection is shown in Figure 3b. The Hessian-based vesselness of the original CCTA image is shown in Figure 3c, which is a bit narrower. Therefore, the edges detected by the Sobel operator show different and incorrect edges, as shown in Figure 3d. Hence, in order to obtain correct edges, we performed thresholding on Frangi's response with respect to quantile and median values.

Quantile was used to determine voxels with Frangi's response with a 98% significance. This method was chosen because almost 90% of responses in Hessian-based vesselness are almost zero. Generally, it is assumed that voxels belonging to tubular or circular components have similar vesselness responses. Therefore, a vesselness response with 80% of the median vesselness response was thresholded by exploiting spatial and temporal similarity. The results of the thresholded Frangi's response and its respective Sobel edge detection are shown in Figures 3e and 3f, respectively.

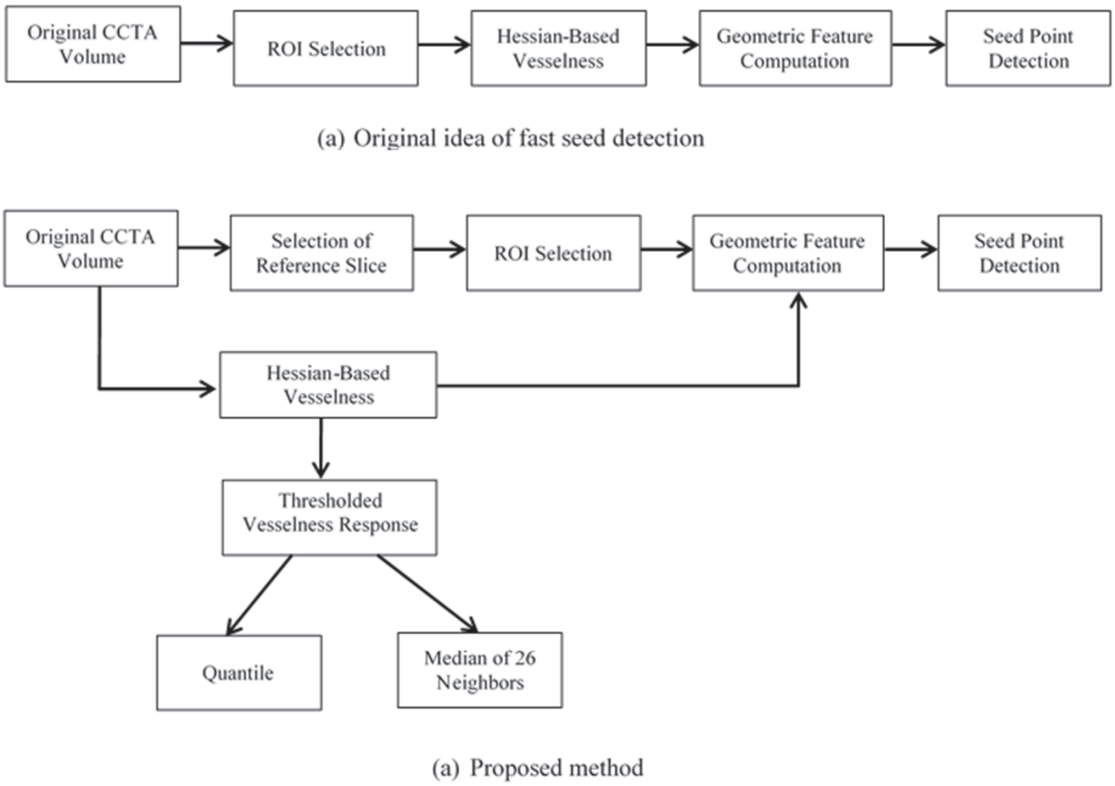

Figure 2. Block diagram of the original method and the proposed method.

Another similar example is shown in Figure 4. This example compares Frangi's response and a thresholded Frangi's response for a case when the component of the coronary artery is located at the border of the heart region, as indicated by the green box in Figure 4a. The Sobel edge detector is not able to detect the edges accurately, as shown in Figure 4b. When the edge detector is applied to Frangi's response, as shown in Figure 4c, the edges are detected, but with an inaccurate and contracted shape, as shown in Figure 4d. This is because Hessian-based vesselness finds it difficult to detect true vessel features at the boundary of the vessel. As a result, the shape of the vessel becomes contracted from the boundary, compared to its original shape. However, when edge detection is applied to the thresholded Frangi's response, as shown in Figure 4e, the edges are detected accurately, as shown in Figure 4f.

After thresholding the Frangi response, the ROI selection procedure and geometric feature computation are applied, as explained in Section 2.2.

4. Experimental results

To illustrate the effectiveness of the proposed method in improving fast seed detection, we applied the proposed method to nine CCTA datasets. Each dataset consists of slices in the range from 250 to 350, with a matrix size of 512×512 for each dataset.

Our aim was to select an axial slice that was guaranteed to contain parts of all major coronary arteries. An axial slice obtained using Eq. (3) depends upon the value of constant c_r, which defines the relative position of an axial slice. The values of $c_r = [0.25, 0.30, 0.35, 0.40, 0.45, 0.50, 0.55, 0.60]$ were used for the selection of

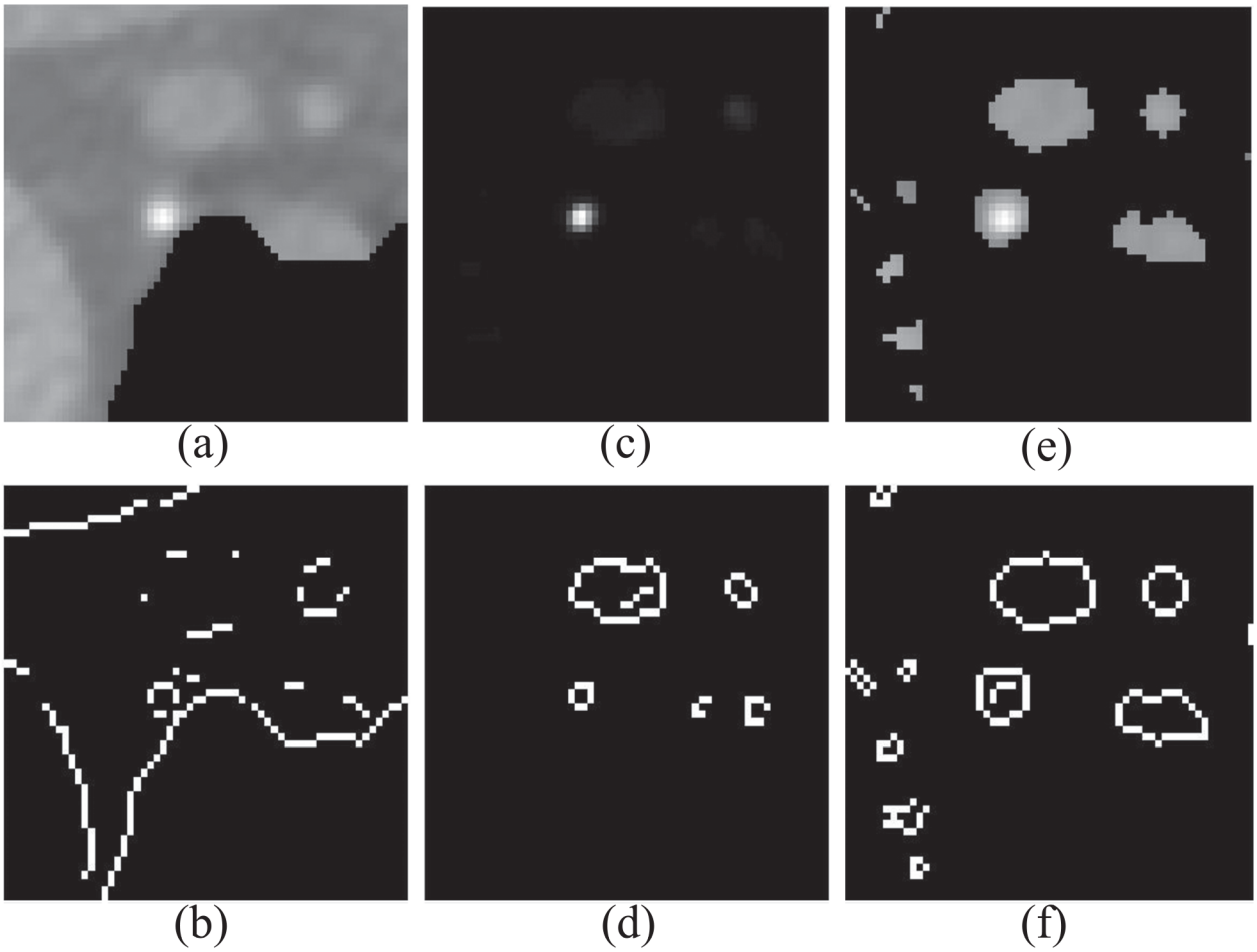

Figure 3. Original CCTA slice with Frangi and thresholded Frangi responses. (a) Original slice from CCTA. (b) The result of Sobel edge detection applied to (a). (c) Hessian-based vesselness of (a). (d) The result of Sobel edge detection applied to (c). (e) Thresholded Frangi response with respect to quantile and median values. (f) Result of Sobel edge detection applied to (e).

eight slices from each dataset systematically. To validate our results, the detected seed points were verified by a radiologist. According to the comments and evaluation by the radiologist, the seeds detected by the proposed method were accurate coronary seed points with fewer or negligible false detections than Han's method [9]. In all the experiments, Hessian-based vesselness responses were generated by using the values 0.6, 0.5, and 220 for alpha, beta, and gamma, respectively. Hessian-based vesselness was obtained using scales ranging from 2 to 5. The experimental results shown in Figure 5 demonstrate the usefulness of the proposed method for improved fast seed point detection. Figure 5 shows the results for a randomly selected volume out of nine clinical datasets.

First, an axial slice showing parts of the major coronaries is selected and then the proposed robust fast seed detection procedure is applied. For our experiments, thresholds T_F and T_{GF} were set to 0.0019 and 14, respectively. The values of T_F and T_{GF} are selected by analyzing the vesselness response and geometrical feature response of all ground truth seed points for all selected slices, and the minimum values are selected as thresholds for the entire dataset. Figure 5a represents the original axial slice with the coronary seed point regions marked by green circles. These green circles show the presence of three main coronary artery components.

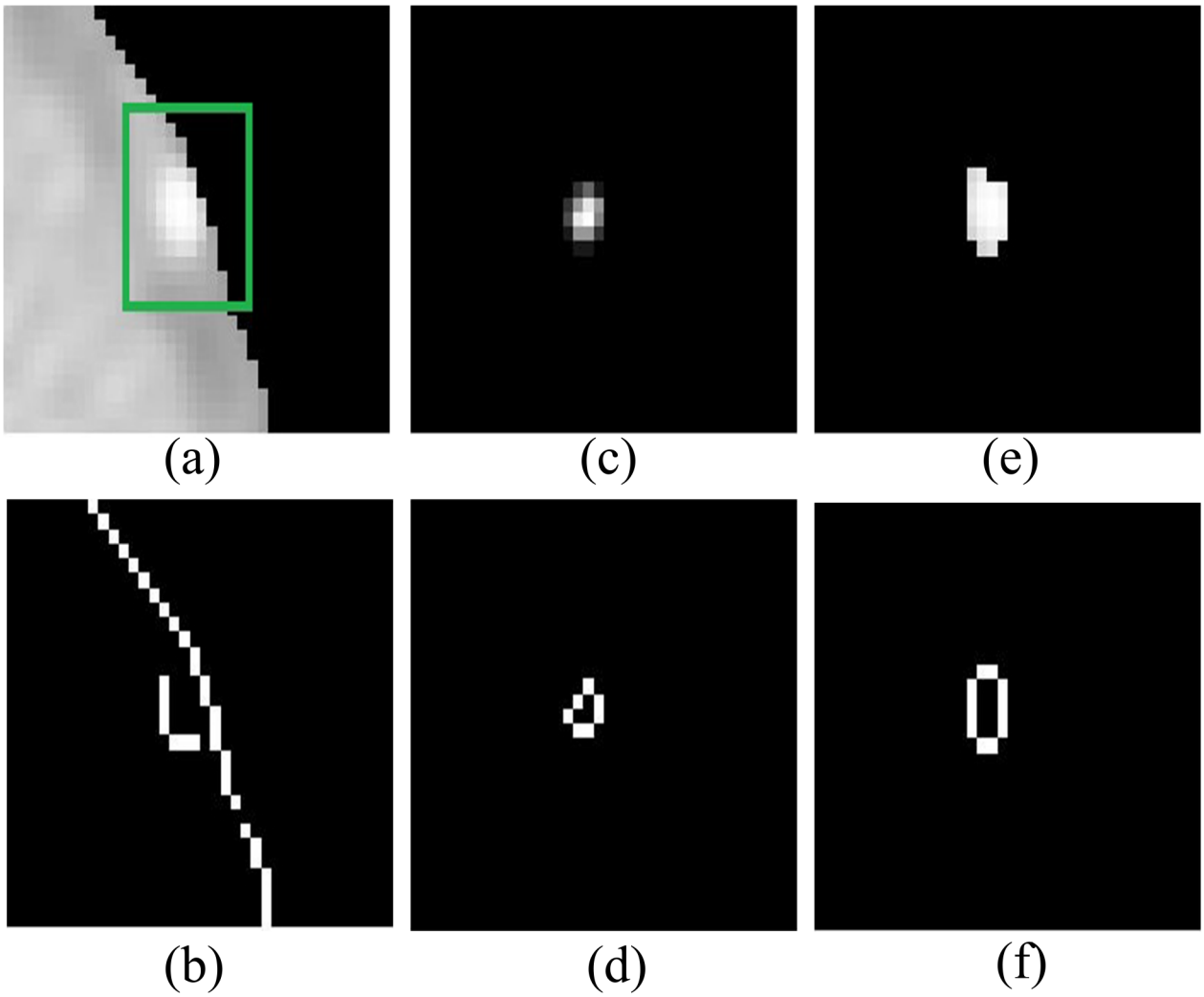

Figure 4. Original CCTA slice with the Frangi and thresholded Frangi responses showing seed points at the border. (a) Original slice from CCTA. (b) The result of Sobel edge detection applied to (a). (c) Hessian-based vesselness of (a). (d) The result of Sobel edge detection applied to (c). (e) Thresholded Frangi response with respect to quantile and median values. (f) The result of Sobel edge detection applied to (e).

Figure 5b shows the seeds detected by Han's method, whereas Figure 5c shows the seed points detected by the proposed method. As seen in CCTA slices shown in Figure 5b, Han's method was unable to detect all potential seed points of the left as well as right coronary arteries, whereas the proposed method successfully detects all coronary seed points correctly for both left and right coronary arteries, as shown in Figure 5c.

It is also noted that, in the first row of Figure 5, a different behavior is illustrated by Han's method, where it was unable to detect any of the potential seed points for both left and right coronary arteries; furthermore, it detected wrong seed points due to the step-edge response introduced by the Hessian-based vesselness filter. In contrast, the proposed algorithm was able to detect all seeds representing components of all major coronary arteries. Our method did not detect a bright circular region marked by t yellow box in the last image in the right column of Figure 5. Although it looks similar to the coronary seed point, it is not actually the seed point.

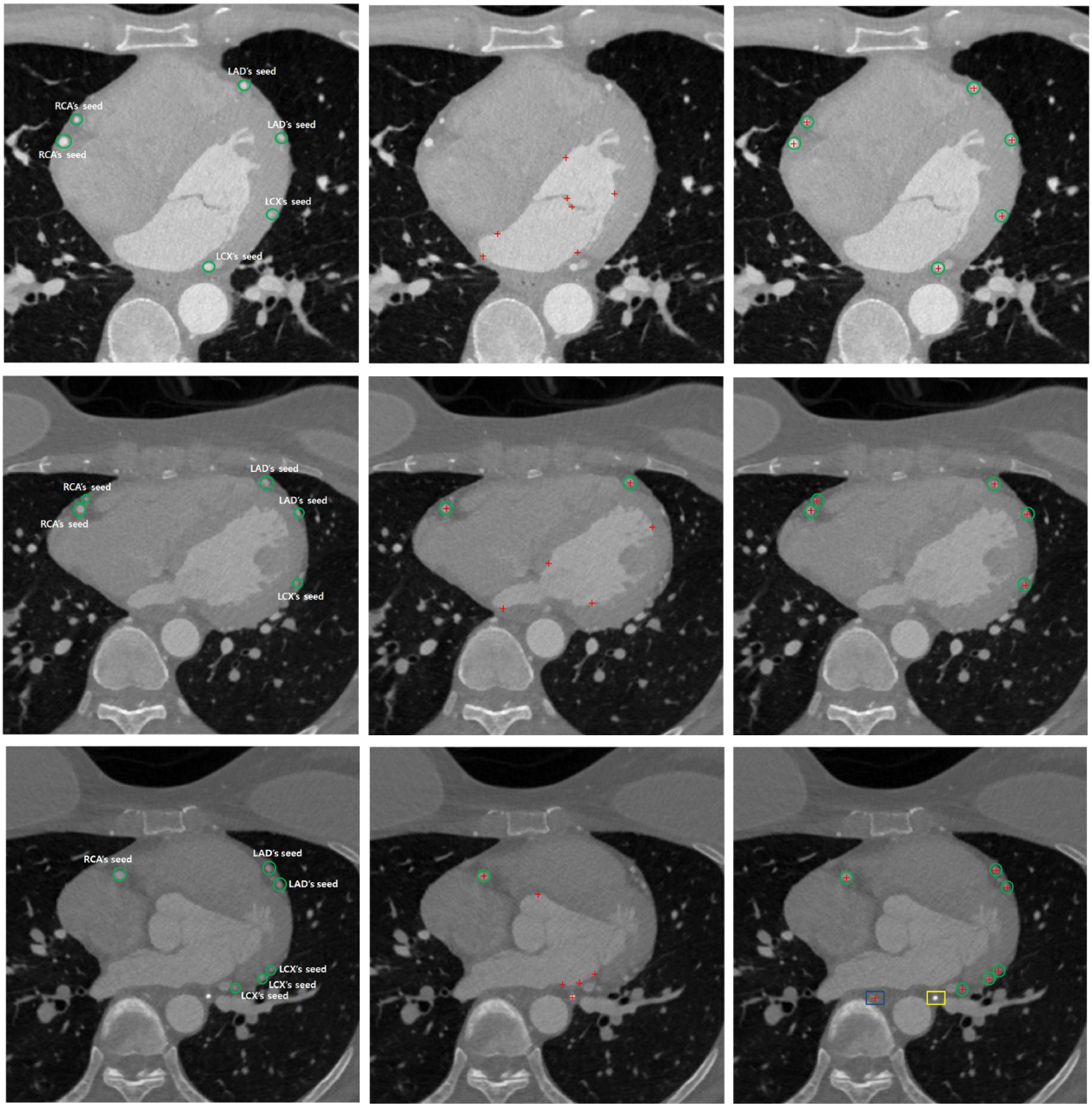

Figure 5. Results of seed detection. (a) Original axial slice. (b) Han's method [9]. (c) Proposed method.

This false seed is not being detected due to the proposed thresholding of Frangi vesselness. On the other hand, Han's approach falsely detected this region as a coronary seed point. The area marked by the blue box in Figure 5 indicates a failure case of the proposed algorithm, where our method detected one seed that did not belong to any of the three major coronary arteries. This was because the Frangi vesselness response and geometrical feature response for this particular region were similar to vessel components. That is why our algorithm is unable to distinguish between the vessel and nonvessel component in this specific case.

To check the accuracy of the proposed method, we selected axial slices systematically using Eq. (1) for different datasets. Bar graphs were generated to show their accuracy, as shown in Figure 6. Figure 6 clearly shows that the proposed method outperformed the previous method in accuracy computed at the individual slice level. This accuracy is measured in terms of number of true detections of coronary artery seeds. The last graph in Figure 6 shows that Han's method completely failed to detect any of the coronary seed points in slice number 179.

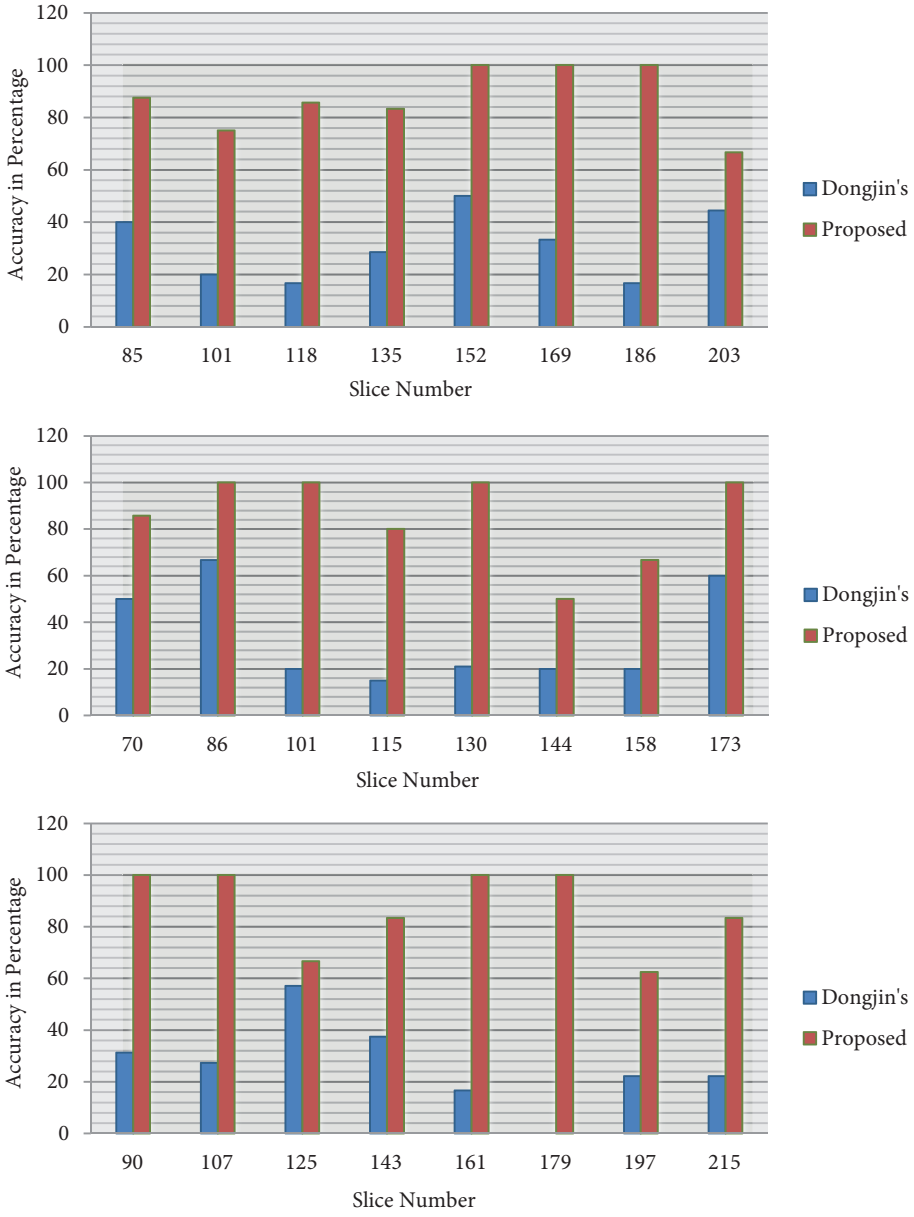

Figure 6. Accuracy for three randomly selected datasets.

Figure 7 compares the proposed method with Han's. This comparison was performed with respect to the average accuracy for five datasets, which were selected randomly. The green bar in Figure 7 shows the superior performance of our method.

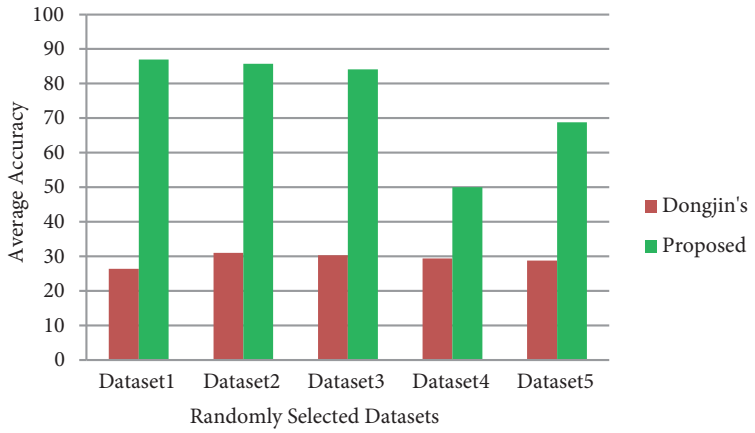

Figure 7. Average accuracy of five randomly selected datasets.

To further demonstrate the performance quantitatively, the Table shows the average accuracy values, in percentages, for Han's method and the proposed method. The proposed method achieved a 45.9% overall improvement compared to the previous method.

Table. The average accuracy for different datasets.

Datasets	Average accuracy (%)	
Dataset 1	26.4	86.9
Dataset 2	31.0	85.7
Dataset 3	30.3	84.0
Dataset 4	29.4	50.0
Dataset 5	28.7	68.8
Average	29.2	75.1

5. Discussion

A robust fast seed detection technique that can be used for efficiently delineating the coronary arterial tree from CCTA images in an automatic fashion is presented. The method is based on the thresholding applied to the Frangi's response [10]. One big disadvantage of the Hessian-based vesselness filter is strong step-edge responses at nonvessel voxels of cardiac chambers boundaries, which have similar CT density values to coronary arteries in CCTA. To reduce the number of false positives due to step-edge response in the existing Hessian-based vesselness, thresholding with respect to quantile and median values is applied and then ROI selection is employed on this scrutinized vesselness response. Furthermore, the proposed thresholded Hessian-based vesselness response is combined with the local geometric feature to accurately detect the coronary seed points. Han et al. [9] also combined the local geometric feature with Hessian-based vesselness for better overall performance, but due to the step-edge response of Hessian-based vesselness and the use of the Sobel operator for detecting edges in the selected regions, this method may lose some of the potential coronary artery components that are located at the boundary of the heart zone.

Another advantage of the proposed method is that we have selected multiple axial slices in a systematic way and then applied the proposed seed detection procedure, which produced more accurate results than Han's method [9].

6. Conclusion

In this paper, an improved and robust fast seed detection method was developed that can be used by any region-based algorithm for segmenting coronary arteries from CCTA images. Since the use of the Sobel operator and morphological operations can cause potential coronary seeds to be discarded during shape analysis, the Hessian-based vesselness measure is computed before the shape analysis procedure. We have also proposed thresholding Hessian-based vesselness with respect to median and quantile values to detect the vessel features accurately for boundary pixels. Seed points representing three main coronary arteries were detected accurately using the proposed method. The performance of the proposed method was evaluated and validated in nine clinical datasets by a radiologist. On average, this method has achieved 45.9% improvement over the previous method.

Acknowledgment

The authors are highly grateful to Dr Soon-Yong Song and Dr Jong-Hyun Lee, Department of Radiology, Hanyang University Seoul Hospital, South Korea, for providing the CCTA datasets and their valuable clinical evaluation throughout the research.

References

[1] Li Z, Zhang Y, Liu G, Shao H, Li W, Tang X. A robust coronary artery identification and centerline extraction method in angiographies. Biomed Signal Proces 2015; 16: 1-8.

[2] Florin C, Paragios N, Williams J. Particle filters, a quasi-Monte Carlo solution for segmentation of coronaries. In: Duncan JS, Gerig G, editors. Medical Image Computing and Computer-Assisted Intervention – MICCAI 2005. MICCAI 2005. Lecture Notes in Computer Science, Vol. 3749. Berlin, Germany: Springer.

[3] Schaap M, Smal I, Metz C, Van Walsum T, Niessen W. Bayesian tracking of elongated structures in 3D images. Inf Process Med Imaging 2007; 20: 74-85.

[4] Lankton S, Stillman A, Raggi P, Tannenbaum AR. Soft plaque detection and automatic vessel segmentation. In: Proceedings of Medical Image Computing and Computer Assisted Intervention (MICCAI) Workshop: Probabilistic Models for Medical Image Analysis; September 2009; London, UK. pp.1-9.

[5] Kitslaar PH, Frenay M, Oost E, Dijkstra J, Stoel B, Reiber J. Connected component and morphology based extraction of arterial centerlines of the heart (CocomoBeach). The MIDAS Journal: MICCAI Workshop–Grand Challenge Coronary Artery Tracking; 2008.

[6] Bauer C, Bischof H. Edge based tube detection for coronary artery centerline extraction. Insight J 2008.

[7] Kitamura Y, Li Y, Ito W. Automatic coronary extraction by supervised detection and shape matching. In: Proceedings of the IEEE International Symposium on Biomedical Imaging: From Nano to Macro; May 2012. pp. 234-237.

[8] Zambal S, Hladuvka J, Kanitsar A, Buhler K. Shape and appearance models for automatic coronary artery tracking. In: Medical Image Computing and Computer-Assisted Intervention–MICCAI Workshop: 3D Segmentation in the Clinic: A Grand Challenge II; 2008.

[9] Han D, Doan NT, Shim H, Jeon B, Lee H, Hong Y, Chang HJ. A fast seed detection using local geometrical feature for automatic tracking of coronary arteries in CTA. Comput Meth Prog Bio 2014; 117: 179-188.

[10] Frangi AF, Niessen WJ, Vincken KL, Viergever MA. Multiscale vessel enhancement filtering. In: Wells WM, Colchester A, Delp S, editors. Medical Image Computing and Computer-Assisted Intervention — MICCAI'98. MICCAI 1998. Lecture Notes in Computer Science, Vol. 1496. Berlin, Germany: Springer .

[11] Wang Y. Blood vessel segmentation and shape analysis for quantification of coronary artery stenosis in CT angiography. PhD, City University, London, UK, 2011.

[12] Tsai YC, Lee HJ, Chen MYC. Automatic segmentation of vessels from angiogram sequences using adaptive feature transformation. Comput Biol Med 2015; 62: 239-253.